Chaos, Solitons and Fractals 193 (2025) 116069

Contents lists available at ScienceDirect

Chaos, Solitons and Fractals

journal homepage: www.elsevier.com/locate/chaos

Anomalous complete synchronization in relay oscillators

Ranjib Banerjee [a,*], Sayan Acharya [b], Matjaž Perc [c,d,e,f,g], Dibakar Ghosh [b]

[a] School of Engineering and Technology, BML Munjal University, Gurugram, 122413, Haryana, India
[b] Physics and Applied Mathematics Unit, Indian Statistical Institute, 203 B. T. Road, Kolkata 700108, India
[c] Faculty of Natural Sciences and Mathematics, University of Maribor, Koroška cesta 160, 2000 Maribor, Slovenia
[d] Community Healthcare Center Dr. Adolf Drolc Maribor, Ulica talcev 9, 2000 Maribor, Slovenia
[e] Complexity Science Hub Vienna, Josefstädterstraße 39, 1080 Vienna, Austria
[f] Department of Physics, Kyung Hee University, 26 Kyungheedae-ro, Dongdaemun-gu, Seoul 02447, Republic of Korea
[g] University College, Korea University, 145 Anam-ro, Seongbuk-gu, Seoul 02841, Republic of Korea

ARTICLE INFO

Keywords:
Anomalous complete synchronization
Generalized synchronization
Dynamical relay coupling
Enhancing synchrony

ABSTRACT

In the past, anomalous phase synchronization was observed analytically and experimentally between two nonidentical chaotic oscillators. In this work, we consider a chain of mutually coupled three oscillators where heterogeneity (in terms of parameter mismatch) is introduced in the middle (relay) oscillator, and the outer two oscillators are identical. We observe an anomalous complete synchronization between the outer oscillators. A common time-delay between the identical outer oscillators and the mismatched relay oscillator plays an important role for the emergence of anomalous complete synchrony. We present several example systems to verify our results with and without coupling delay. We also observe generalized synchronization between the relay oscillator and the outer identical oscillators. The variation of parameter mismatch, coupling strength and coupling delay on the anomalous complete synchronization is studied with diffusive and globally coupled network.

1. Introduction

Synchronization is a natural phenomenon for coupled chaotic dynamical systems [1]. Among all types of synchronization, complete synchronization (CS) is the most commonly found phenomenon in coupled dynamical systems, in which the coupled oscillators gradually start catching up with the common rhythm as the coupling strength increases. Synchronization applications are available in various domains, including signal processing [2,3], power grid [4], traffic network [5], brain network [6], etc. A wide variety of coupling configurations have been used to establish different types of synchronization phenomena. The study of remote synchronization using indirect/relay coupling is an important issue in recent days [7–10]. Instead of direct interaction, two or more oscillators are allowed to interact via an intermediate oscillator in this mechanism. Remote synchrony is observed in a multiple connected star graph to understand collective phenomena of distant connections of brain networks [11]. Also the role of hub in the start network for the remote synchronization is discussed by Vladimir et al. [12]. The existence of more general collective states is explored for arbitrary network topologies, i.e., for complex networks [13]. Recently, Rakshit et al. [14] introduced the concept of relay interlayer synchronization between two equidistant identical layers which are coupled via a mismatched relay layer. Later, the relay synchronization is also observed in triplex networks with degree-based mechanism [15].

In our previous works [16,17], we explored the role of heterogeneity in enhancing the complete synchronization between the identical oscillators using a relay model. We reported that the presence of heterogeneity in terms of the parameter mismatch in the mediating oscillator(s) plays a crucial role in the enhancement of CS between the symmetrically placed oscillators in various configurations. The above result has been established in both one- and two-dimensional lattices, star and ring networks using different chaotic oscillators governing the dynamics of individual node. Experimental verification of the enhancement of complete synchronization has been done with the help of electronic circuit of chaotic Rössler oscillator [16]. The phenomenon of enhancement of CS can only be found using the above mechanism when the interacting oscillators are in their chaotic regime. However, the opposite phenomenon (de-enhancement) is observed when the individual oscillators are in periodic/limit cycle (LC) states, mainly because the CS is achieved at a very low coupling strength for coupled LC oscillators [16]. Further investigation revealed that the synchronization error between the outer oscillators (or symmetrically placed oscillators depending on the configuration scheme) increases first for low coupling

* Corresponding author.
E-mail address: ranjib.banerjee@bmu.edu.in (R. Banerjee).

https://doi.org/10.1016/j.chaos.2025.116069
Received 24 December 2024; Accepted 23 January 2025

strength before settling down to the complete synchronization state (synchronization error decreases to zero) for higher coupling strength. This phenomenon is found generic for variety of oscillators including Rössler oscillator, Lorenz oscillator, Mackey–Glass delay model etc. As it can only be observed on the onset of CS between identical chaotic oscillators, we call this phenomenon anomalous complete synchronization (ACS) state. The transition from disordered to phase synchronized state is often a monotonic process. The frequency difference between oscillators diminishes as coupling strength increases. Nonlinear oscillators have non-isochronous properties and asymmetric coupling, causing greater coupling to progressively raise the frequency difference before decreasing it to zero. This non-monotonic approach, known as anomalous phase synchronization (APS). In previous studies [18,19], APS is observed in nonidentical phase oscillators owing to the lack of synchronicity in the system, which was later experimentally verified by Dana et al. [20] using the electronic circuits of coupled Chua oscillators. In 2008, Prasad et al. [21] discussed the effect of time delay on anomalous synchronization. In the same year, Tokuda et al. [22] detected the anomalous synchronization using the time series of two oscillators. In addition to anomalous synchronization [23], enhancing synchronization is also observed using the optimal time-varying function.

In most of the previous works [18–23], the anomalous phase synchronization is observed and little attention has been paid on complete synchronization. In this work, we show the ACS effect in two indirectly coupled identical oscillators (Oscillator 1 & 3) in chaotic and limit cycle regimes in a linear array of three mutually coupled oscillators as shown in Fig. 1. The rest of the paper is organized as follows:

The ACS is shown for coupled Rössler model in Section 2.1 and Lorenz models (Appendix A.1) in their chaotic regimes. Generalized synchronization (GS) between the mediating oscillator (Oscillator 2) and one of the end-oscillators (Oscillator 1) is presented in Section 2.2. Subsequently, we demonstrate the ACS phenomenon for the coupled Rössler and Mackey–Glass time-delay model with coupling delay in Section 3. Stability analysis of ACS using the Krasovskii–Lyapunov theory is shown in Section 4. We further illustrate the ACS phenomenon for coupled Rössler oscillators applying global network in each layer in Section 5. We conclude our findings in Section 6. In Sec. Appendix A.1, we present some additional results on ACS using chaotic Lorenz oscillator, and limit cycle Ginzburg–Landau model (Sec. Appendix A.2).

2. Three oscillators with instantaneous coupling function

To show the ACS phenomena, we first consider three oscillators coupled in an open chain, the outer two oscillators are identical and heterogeneity in terms of parameter mismatch is introduced in the relay oscillator. The schematic representation is shown in Fig. 1. Here, the outer identical oscillators 1 and 3 (solid circle) are indirectly coupled through the mismatched relay oscillator 2 (dashed circle).

2.1. Three coupled chaotic oscillators

We investigate the effect of the heterogeneity present in the relay oscillator in form of parameter mismatch when three oscillators are mutually coupled in an open-ended linear array. We present the result for three Rössler oscillators for different sets of parameter values: once in the chaotic regime and then in the limit cycle regime. The mathematical formulation of the coupled system is given below,

Outer oscillators:

$$\begin{aligned} \dot{x}_{1,3} &= -\omega y_{1,3} - z_{1,3} + \epsilon(x_2 - x_{1,3}), \\ \dot{y}_{1,3} &= \omega x_{1,3} + a y_{1,3}, \\ \dot{z}_{1,3} &= b + (x_{1,3} - c) z_{1,3}, \end{aligned} \tag{1}$$

Relay oscillator:

$$\begin{aligned} \dot{x}_2 &= -(\omega + \Delta\omega) y_2 - z_2 \\ &\quad + \epsilon(x_1 + x_3 - 2x_2), \\ \dot{y}_2 &= (\omega + \Delta\omega) x_2 + a y_2, \\ \dot{z}_2 &= b + (x_2 - c) z_2, \end{aligned} \tag{2}$$

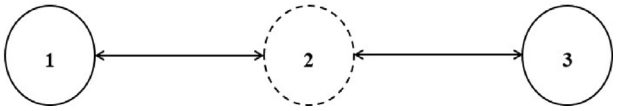

Fig. 1. One dimensional lattice of three linearly coupled oscillators. The solid and dotted circle respectively indicate identical and mismatched oscillator.

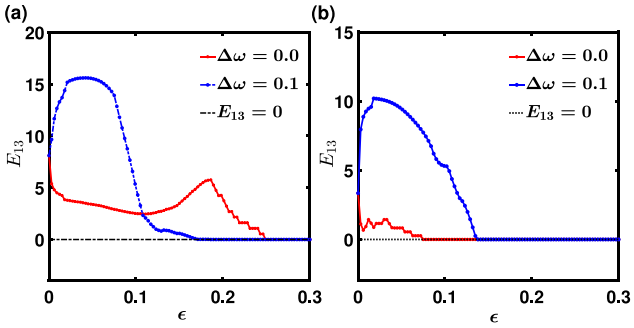

Fig. 2. Synchronization error between the outer oscillators is plotted against the coupling strength (ϵ) for three diffusively coupled Rössler oscillators as represented by Eq. (1). For figures (*a&b*), we choose the initial conditions $(x, y, z) \in [-10, 10] \times [-10, 10] \times [0, 20]$ and parameter values as $a = 0.2$, $b = 0.4$, $c = 7.0$ from the chaotic regime and parameter values $a = 0.2$, $b = 0.2$, $c = 3.5$ from the limit cycle regime of Rössler oscillator, respectively. For both cases, red dotted line and blue dash-dotted line indicate error (E_{13}) without mismatch $\Delta\omega = 0.0$, with mismatch $\Delta\omega = 0.1$ respectively and $\omega = 1.0$. Anomalous synchronization behavior can be observed in the presence of the parameter mismatch ($\Delta\omega \neq 0$) in the mediating oscillator. In the presence of parameter mismatch, as the coupling strength increases the synchronization error between the outer oscillators shoots up initially and then reduces to zero. We observe that without parameter mismatch, the enhancing errors arise when parameter values are chosen from the chaotic regime, while situations reducing errors occur when values are drawn from the limit cycle regime.

where ϵ represents the coupling strength and $\Delta\omega$ is the amount of mismatch in ω in the relay oscillator. Each uncoupled oscillator (i.e., for $\epsilon = 0$) is in chaotic state for $a = 0.2, b = 0.4$ and $c = 7.0$.

We observe that the synchronization error between the outer oscillators E_{13} (as defined in Eq. (3)) gradually reduces with respect to the coupling strength when all three oscillators are identical (i.e., $\Delta\omega = 0.0$) in both the chaotic and the limit cycle cases (Fig. 2). However, as soon as the mismatch is introduced ($\Delta\omega \neq 0.0$) in the relay oscillator, the same synchronization error is found to increase in the beginning before settling down to zero. The time averaged synchronization error between outer oscillators (oscillator i&j) is defined as

$$E_{ij} = \left\langle \sqrt{(x_i - x_j)^2 + (y_i - y_j)^2 + (z_i - z_j)^2} \right\rangle_t, \tag{3}$$

is plotted against the coupling strength (ϵ) in Fig. 2, where $\langle \ldots \rangle_t$ is used to denote the time average of the synchronization error. The red dotted line represents the synchronization error when all three oscillators are identical (i.e., $\Delta\omega = 0$) which follows an expected route to falls slowly until securing the complete synchronization ($E_{13} = 0$) between them beyond a threshold coupling strength. However, with mismatch ($\Delta\omega \neq 0$) in the relay oscillator (Oscillator 2 in Fig. 1), the synchronization error shows anomaly in its behavior; first increases with coupling strength and then reduces towards zero, as shown in blue dash-dotted line in Fig. 2 for $\Delta\omega = 0.1$. For numerical simulations, we use RK-45 method with step size $h = 0.01$ with 10^7 time iteration. Error is calculated from last 20% data of time iteration.

This behavior and mechanism are not reported before for complete synchronization, which we find counterintuitive to the existing notions

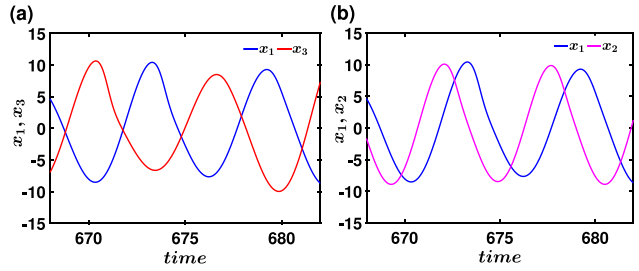

Fig. 3. The time series of x_1, x_3 and x_1, x_2 is plotted in (a) and (b), respectively, in the presence of parameter mismatch $\Delta\omega = 0.1$ with fixed coupling strength $\epsilon = 0.04$. Each case parameters value $a = 0.2$, $b = 0.4$, $c = 7.0$ from chaotic regime of Rössler system. Blue, magenta and red lines represent the time series of x_1, x_2 and x_3, respectively. Initial conditions are picked randomly from the basin of attractions. We plainly note that x_1, x_3 are close to anti-phase in (a), whereas x_1, x_2 indicate just a slight lag in (b).

and hence report in this manuscript. In order to understand the underlying mechanism of this anomalous route to complete synchronization, we plot the time series x_1, x_3 for various coupling strengths (ϵ) with parameter mismatch. However, we present only the time series of x_1, x_3 and x_1, x_2 as illustrated in Fig. 3 when the error E_{13} reaches its peak for $\epsilon = 0.04$ with parameter mismatch $\Delta\omega = 0.1$. From Fig. 3 (a), we analyze that $x_1 - x_3$ is almost in anti-phase state and $x_1 - x_2$ maintain a lag. As we increase the coupling strength ϵ beyond 0.04, the synchronization error diminishes and the phase relationship between x_1 and x_3 shifts. Around $\epsilon = 0.2$, complete synchronization emerges ($E_{13} = 0.0$), with x_1 and x_3 being in phase, while x_1 and x_2 still exhibit a slight lag.

2.2. Generalized synchronization between relay and outer oscillators

So far, we notice that once a critical coupling strength $\epsilon_c = 0.17$ is attained, the outer oscillators are completely synchronized. Now we will show that at the same critical coupling strength, generalized synchronization (GS) appears between the relay oscillator and any one of the outer oscillators. Theoretically, for two dynamical systems whose dynamics are defined by the equations $\dot{x}(t) = f(x(t), y(t))$ and $\dot{y}(t) = g(y(t), x(t))$, GS relies on the existence of a one-to-one function $h(x(t))$ such that $\lim_{t\to\infty} \|y(t) - h(x(t))\| = 0$ [24,25]. In our case for GS on the system (1), there is a possibility that a functional relationship $X_{1,3} = h(X_2(t))$ exists but determining the explicit form of $h(X)$ is practically very challenging. So, to observe GS, we plot the entire Lyapunov spectrum of the coupled systems and the synchronization error as a function of the coupling strength (ϵ). From Fig. 4(a), we see that beyond a critical value of the coupling strength $\epsilon_c \approx 0.17$, the synchronization error between outer oscillators (E_{13}) goes to zero whereas the error between outer and relay oscillator (E_{12}) still remains positive, which makes it clear that CS occurs between the outer oscillators above this critical coupling strength. To visualize GS state, we compute the entire Lyapunov spectrum of the full nine-dimensional system (1). The six largest Lyapunov exponents ($\lambda_1 \geq \lambda_2 \geq \lambda_3 \geq \lambda_4 \geq \lambda_5 \geq \lambda_6$) in the spectrum are plotted as a function of coupling strength ϵ in the Fig. 4(b). For very low coupling strength, three Lyapunov exponents $\lambda_1, \lambda_2, \lambda_3$ are positive, three $\lambda_4 = \lambda_5 = \lambda_6$ are exactly equal to zero and three $\lambda_7, \lambda_8, \lambda_9$ are less than zero (i.e., $\lambda_1 \geq \lambda_2 \geq \lambda_3 > 0, \lambda_4 = \lambda_5 = \lambda_6 = 0, 0 > \lambda_7 \geq \lambda_8 \geq \lambda_9$). As the coupling strength increases, λ_6 drops to value below zero ($\lambda_6 < 0$). If we plot phase-space orbits of the systems, we notice that phase synchronization occurs between the outer oscillators at this stage. With slight increase in the coupling strength, λ_5 becomes negative ($\lambda_5 < 0$) and λ_3 vanishes. So far in our system (1), two largest Lyapunov exponents are positive ($\lambda_1, \lambda_2 > 0$), the two Lyapunov exponents λ_3, λ_4 are equal to zero and the rest of all are negative, which suggests that two chaotic amplitudes are not correlated. The further increase in the coupling strength, λ_4 drops below zero, eventually reaching higher coupling strength λ_3 becomes negative and λ_2 drops

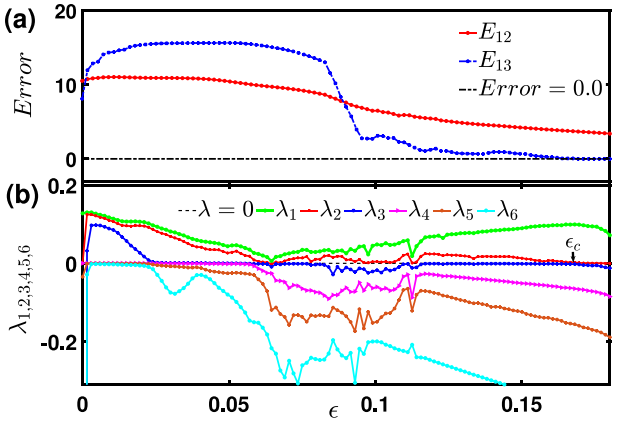

Fig. 4. (a) In the presence of parameter mismatch ($\Delta\omega = 0.1$) in relay oscillator, variation of synchronization error E_{13} (see text Eq. (3) for definition) between outer oscillators (blue-dashed dotted line) and between relay and outer oscillators E_{12} (red-dotted line) as a function of coupling strength ϵ. For numerical simulation, we use RK-45 method for time $t = 10^7$ and step size 0.01. (b) Variation of the entire Lyapunov spectrum as a function of coupling strength ϵ of the coupled system (1). The six largest Lyapunov exponents (λ_i) for $i = 1, 2, \ldots, 6$ are shown out of nine Lyapunov exponents and the rest three Lyapunov exponents are negative always. As coupling strength attains critical value (ϵ_c), $\lambda_1 > 0, \lambda_2 = 0, \lambda_i < 0$ (for $i = 3, 4, 5, 6$) indicating the existence of the GS state between relay and outer oscillators and at the same time, CS state between outer oscillators. From figure (a) and (b) it is very clear that $\epsilon = \epsilon_c = 0.17$ is the critical coupling strength where CS occurs between outer oscillators and GS occurs between relay and outer oscillators. From both figures it is pretty clear that at the critical coupling strength ϵ_c, the synchronization error (E_{13}) of the outer oscillators goes to zero and all the Lyapunov exponents except first and second largest Lyapunov exponents ($\lambda_1 > 0, \lambda_2 = 0$) become negative resulting that GS emerges for $\epsilon > \epsilon_c$.

to zero. If we look closely in the regime $\epsilon = 0.17 \pm 0.001$, one largest Lyapunov exponent λ_1 is positive, λ_2 is exactly equal to zero and $\lambda_i < 0$ for $i = 3, 4, \ldots, 9$ indicating only one independent chaotic amplitude in the whole system (1), also the regime is almost perfectly matched with critical coupling strength ϵ_c in the Fig. 4(a). Such indications suggest that GS takes place between any of the outer oscillators with the relay oscillator [26].

3. Identical systems with time-delay coupling functions

Next, we consider identical oscillators and introduce a time delay in the coupling. The delay differential equation (DDE) has been studied for the last 200 years [27]. In the 18th century, the delay differential equation was initially introduced by Laplace and Condorcet [28]. However, after the second world war the theory and application of this area developed rapidly and also continues today. Some basic theory on stability and some important works were developed by Pontryagin in 1942, Bellman and Cooke in 1963 [29], Smith in 1957, Halanay in 1966, El'sgol'c and Norkin in 1971 [30], Myshkis in 1972 [31], Yanushevski in 1978 [32] and Hale in 1977 [27].

3.1. Rössler system

In this section, we introduce time delay in the coupling terms and the dynamics of the delay coupled Rössler system can be expressed as follows:

Outer oscillators:

$$\begin{aligned} \dot{x}_{1,3} &= -y_{1,3} - z_{1,3} + \epsilon(x_2(t-\tau) - x_{1,3}), \\ \dot{y}_{1,3} &= x_{1,3} + a y_{1,3}, \\ \dot{z}_{1,3} &= b + (x_{1,3} - c) z_{1,3}, \end{aligned} \tag{4}$$

Relay oscillator:

$$\dot{x}_2 = -y_2 - z_2 + \epsilon(x_1(t-\tau) + x_3(t-\tau) - 2x_2),$$

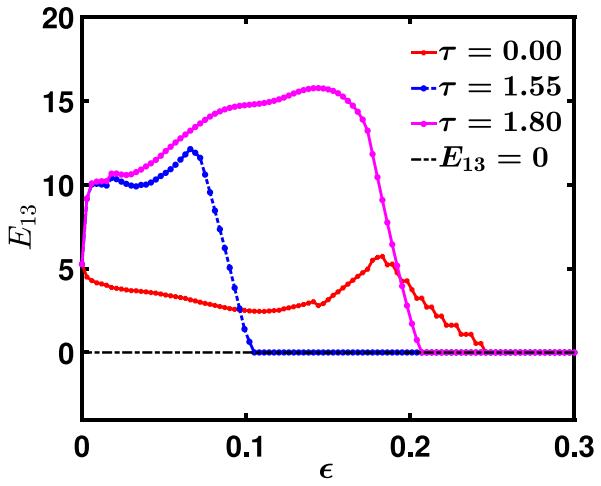

Fig. 5. The graph displays the variation of synchronization error E_{13} between the outer oscillators (i.e., the first and third systems) by changing the coupling strength (ϵ). Here we notice synchronization errors as a result of applying varying time delays. The red dotted, blue dash-dotted, and magenta dotted lines represent the error E_{13} for $\tau = 0.0, \tau = 1.55$, and $\tau = 1.80$, respectively. We integrate system (4) using Heun's method for time $t = 10^7$ with $dt = 0.01$ and E_{13} is the time averaged over last 20% data.

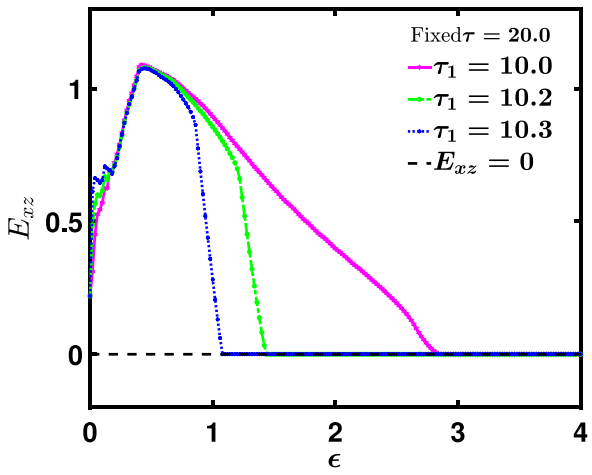

Fig. 6. Fluctuations in synchronization error E_{xz} of outer Mackey–Glass systems as a function of the coupling strength (ϵ). The magenta, green-dotted, and blue-dotted lines represent the synchronization errors of the two outer oscillators of the Mackey–Glass system with delay coupling functions $\tau_1 = 10$, $\tau_1 = 10.2$ and $\tau_1 = 10.3$, respectively. The time-averaged error (E_{xz}) is calculated using the last 20% of 10^7 data. Here we observe how time-averaged error varies for various time delays in coupling function fixing the system time delay $\tau = 20$. That makes more straightforward to understand the influence of different time delays on synchronization error.

$$\begin{aligned} \dot{y}_2 &= x_2 + a y_2, \\ \dot{z}_2 &= b + (x_2 - c) z_2, \end{aligned} \tag{5}$$

where ϵ is the coupling strength, a, b, c are parameters of the system (4) and τ is coupling delay time. The variable x is used to establish the coupling, and constant time delay is added to the x_1, x_2, x_3 variables as a coupling function. For the numerical simulation, we choose the parameter value $a = 0.2$, $b = 0.4$, $c = 7.0$ from the chaotic region of the Rössler system, random initial condition for state variables $(x_1, x_2, x_3) \in [-10, 10]\times[-10, 10]\times[-10, 10]$, $(y_1, y_2, y_3) \in [-10, 10]\times[-10, 10]\times[-10, 10]$, $(z_1, z_2, z_3) \in [0, 20] \times [0, 20] \times [0, 20]$ for $\tau = 0.0$. For non-zero τ, we consider constant history like $x_{delay} = 0.5, x_{delay} = 0.1, x_{delay} = 0.3$. Without time delay ($\tau = 0.0$), the error between the outer oscillators and the coupling strength (ϵ) is as usual, as shown in Fig. 5. Initially ($\epsilon = 0.0$), the error $E_{13} = 5.0$, then it decreases as ϵ increases to approximately $\epsilon = 0.12$. After appearing to exhibit rising behavior at about $\epsilon = 0.18$, it decreases and finally drops to zero near $\epsilon = 0.25$. However, when we fix $\tau = 1.55$ and $\tau = 1.88$, the synchronization error E_{13} begins with 5.0 and rapidly grows around $\epsilon = 0.07$ and $\epsilon = 0.18$ and gradually decays to zero at $\epsilon = 0.1$ and $\epsilon = 0.2$, respectively. These critical values of ϵ are much less compared to the case of instantaneous coupling ($\tau = 0.0$). Thus the similar type of ACS phenomenon can be observed between two identical outer oscillators in linearly coupled three-Rössler model when we introduce time delay in the coupling term and remove the parameter mismatch from the relay oscillator.

3.2. Mackey–Glass systems

In 1977, Michael Mackey and Leon Glass introduced an intriguing non-linear delay model for the dynamics of circulating blood cell concentrations in hematopoiesis, commonly referred to as the "Mackey-Glass equation" [33]. The Mackey–Glass equation may produce a variety of dynamics, from convergence to oscillations with distinct features and even chaotic behavior, making it a standard for the application of novel approaches for nonlinear delay differential equations. Over the decades, many great works of theoretical, numerical, and experiments have been done on different time-delay systems [34]. In the recent study [16], we compose the Mackey–Glass delay equation with delay coupling function as follows

$$\begin{aligned} \dot{x} &= -ax + \tfrac{bx(t-\tau)}{1+x^{10}(t-\tau)} + \epsilon(y(t-\tau_1) - x(t)), \\ \dot{y} &= -ay + \tfrac{by(t-\tau)}{1+y^{10}(t-\tau)} + \epsilon(x(t-\tau_1) + z(t-\tau_1) - 2y(t)), \\ \dot{z} &= -az + \tfrac{bz(t-\tau)}{1+z^{10}(t-\tau)} + \epsilon(y(t-\tau_1) - z(t)), \end{aligned} \tag{6}$$

where a and b are individual system parameters, ϵ is the coupling strength. Here τ and τ_1 are constant delay times for the system and coupling function, respectively. We integrate system (6) using Heun method for time $t = 10^7$ with step size $h = 0.01$. For numerical simulation, we choose the values of the parameters $a = 0.5, b = 2.0$, and $\tau = 20.0$. The constant delay functions for the first, second, and third systems are $x_{delay} = 0.901$, $y_{delay} = 0.35$, $z_{delay} = 0.092$, respectively, and the initial conditions for the three systems are $x(0) = 0.12$, $y(0) = 0.2$, $z(0) = 0.5$. The time average synchronization error E_{xz} between the two outer oscillators is defined as

$$E_{xz} = \left\langle \sqrt{(x-z)^2} \right\rangle_t, \tag{7}$$

where $\langle \ldots \rangle_t$ denotes the time average. As depicted in Fig. 6, it is fascinating to observe that the curves for the synchronization error (E_{xz}) for different τ_1 values begin close to 0.25, swiftly increase, and then decline to zero with the escalation of the coupling strength (ϵ). This result is consistent with the results obtained in the previous section where we introduced a constant positive time delay in the coupling functions, as shown in system (4). The similar phenomenon is observed in delay and the non-delay system.

4. Stability analysis of anomalous complete synchronization

The synchronization error for the system described by system (6) can be analytically determined using the Krasovskii–Lyapunov theory framework, which is the extension of the second Lyapunov method for time delay differential equations [35]. In this section, we want to analytically calculate the critical coupling strength at which synchronization between the outer systems occurs. Let $\Delta = z - x$ be the synchronization error between the outer systems. The evolution equation for the synchronization manifold Δ can be expressed as

$$\dot{\Delta} = \dot{z} - \dot{x} = -(a + \epsilon)\Delta + b f'(x(t-\tau))\Delta_\tau, \tag{8}$$

where $\Delta_\tau = \Delta(t-\tau) = z(t-\tau) - x(t-\tau)$ and $f(x(t)) = \frac{x(t)}{1+x^{10}(t)}$. The stability of the equilibrium point $\Delta = 0$ of the error system (8) guarantees local stability of the synchronization state. By utilizing the Krasovskii–Lyapunov theorem, we formulate a positive definite functional, analogous to the Lyapunov function for standard differential equations, to estimate a sufficient condition for stability, is of the form

$$V(t) = \frac{1}{2}\Delta^2 + \lambda \int_{-\tau}^{0} \Delta^2(t+\xi)d\xi \text{ with } V(0) = 0, \tag{9}$$

where $\lambda > 0$ is an arbitrary positive parameter. If the derivative of the functional $V(t)$ along the trajectory is negative, the equilibrium point (i.e., the origin) of Eq. (9) is stable. The derivative of Eq. (9) along the trajectory of the synchronization manifold (8) can be found as below

$$\begin{aligned} \dot{V}(t) &= -(a+\epsilon)\Delta^2 + bf'(x(t-\tau))\Delta\Delta_\tau + \lambda\Delta^2 - \lambda\Delta_\tau^2 \\ &= -(a+\epsilon-\lambda)\Delta^2 + bf'(x(t-\tau))\Delta\Delta_\tau - \lambda\Delta_\tau^2 \\ &= -\lambda\Delta^2\zeta(X,\lambda), \\ &\text{where } \zeta(X,\lambda) = \tfrac{(a+\epsilon-\lambda)}{\lambda} - \tfrac{bf'(x(t-\tau))}{\lambda}X + X^2, X = \tfrac{\Delta_\tau}{\Delta}. \end{aligned} \tag{10}$$

The Eq. (10) is negatively defined function of the variables Δ and Δ_τ (i.e., $\dot{V}(t) \le 0$) if the following condition holds good

$$\begin{aligned} &4\lambda(a+\epsilon-\lambda) - b^2(f'(x(t-\tau)))^2 > 0, \\ \text{i.e., } &a+\epsilon > \lambda + \frac{b^2}{4\lambda}(f'(x(t-\tau)))^2 = \Psi(\lambda) \text{ (say)}. \end{aligned} \tag{11}$$

Now $\Psi(\lambda)$ attains its minimum value at $\lambda = \frac{|bf'(x(t-\tau))|}{2}$. Therefore, above condition (11) can be expressed as

$$\epsilon > \max|bf'(x(t-\tau))| - a. \tag{12}$$

Maximum value of $|f'(x(t-\tau))|$ can be found when $x(t-\tau) = (11/9)^{(1/10)}$, thus the required condition becomes,

$$\epsilon > |b|\frac{9^2}{40} - a. \tag{13}$$

At the system's parameter $a = 0.5$ and $b = 2.0$, the sufficient condition for synchronization becomes $\epsilon > 3.55$. Fig. 6 shows the numerical value of the synchronization error (E_{xz}) between the outer oscillators reduces to zero when the coupling strength is below 3 (i.e., $\epsilon < 3$). However, analytical calculations suggest that the synchronization can be achieved for $\epsilon > 3.55$. The inconsistency between the analytical results and numerical findings arises because the second Lyapunov method (Krasovskii–Lyapunov) provides a sufficient, but not necessary condition for stability. In conclusion of the stability analysis, we examine the evolutionary equation of synchronization error dynamics ($\dot{\Delta}$) between outer oscillators and find the stability condition of the synchronization error ($\Delta = 0$). From this stability condition, we get a region of $\epsilon > 3.55$ beyond which the anomalous complete synchronization takes place between the outer oscillators.

5. Network of oscillators with relay type coupling

In the previous sections, we observed the anomalous route to complete synchronization between the outer oscillators for three coupled Rössler and Mackey–Glass systems. Now, we aim to examine the same phenomenon using three layers of globally connected N oscillators using relayed interaction. The intralayer interaction among the oscillators is global and the interactions between layers are relay type (so, the two adjacent layers do not have direct interaction but via the intermediate layer only). For this, we consider two cases, one with instantaneous relay coupling and another one with coupling delay in the interlayer connections.

5.1. Global network of coupled Rössler oscillators

Initially, in Section 2.1, we examined three coupled Rössler systems with mismatches in the relay oscillator. Now we explore the global network of Rössler oscillator under relay type coupling [15]. Now, the 3-dimensional coupled Rössler system is associated with the ith node

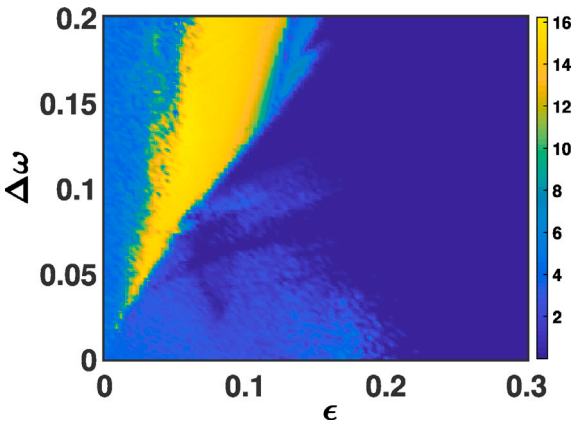

Fig. 7. Error between outer Rössler oscillators (E_{13}) as a function of interlayer coupling strength (ϵ) and mismatch parameter ($\Delta\omega$). For a fixed global coupling strength $\mu = 0.3$, we exhibit parameter space with respect to error E_{13} (in color bar), where mismatch ($\Delta\omega$) varies from 0 to 0.2 and interlayer relay coupling strength ϵ lies on $[0, 0.3]$. Error is defined in Eq. (3). The blue region denotes complete synchronization ($E_{13} = 0.0$), the yellow region represents the maximum error, and the cyan region indicates a non-zero error. The parameter values are picked from the chaotic region of the Rössler oscillator, as detailed in Fig. 2 (*a*). From Fig. 7 we notice that when there is a parameter mismatch in the relay oscillator, the error progressively rises to its maximum and then abruptly falls to zero, unlike the error without mismatch, i.e., the ACS phenomenon is observed clearly.

in the mth layer and its state variable can be represented as the vector $\mathbf{X_{m,i}} \in \mathbb{R}^3$. The mathematical representation of the multiplex network is as follows,

$$\begin{aligned} \dot{\mathbf{X}}_{1,i} &= f(\mathbf{X}_{1,i},\beta) + \mu\textstyle\sum_{j=1}^{N} A_{i,j}^{[1]} G[\mathbf{X}_{1,j} - \mathbf{X}_{1,i}] + \epsilon H[\mathbf{X}_{2,i} - \mathbf{X}_{1,i}], \\ \dot{\mathbf{X}}_{2,i} &= f(\mathbf{X}_{2,i},\beta) + \mu\textstyle\sum_{j=1}^{N} A_{i,j}^{[2]} G[\mathbf{X}_{2,j} - \mathbf{X}_{2,i}] + \epsilon H[\mathbf{X}_{3,i} + \mathbf{X}_{1,i} - 2\mathbf{X}_{2,i}], \\ \dot{\mathbf{X}}_{3,i} &= f(\mathbf{X}_{3,i},\beta) + \mu\textstyle\sum_{j=1}^{N} A_{i,j}^{[3]} G[\mathbf{X}_{3,j} - \mathbf{X}_{3,i}] + \epsilon H[\mathbf{X}_{2,i} - \mathbf{X}_{3,i}], \end{aligned} \tag{14}$$

where $i = 1, 2, \ldots, N$ be the oscillator index in each layer, $f : \mathbb{R}^3 \times \mathbb{R} \to \mathbb{R}^3$ be the evolution function for Rössler oscillator, β is the system parameters. Here μ and ϵ are the intralayer and interlayer coupling strengths, respectively, H represents the inner coupling matrix between layers, which determines the interaction between nodes of one layer and their corresponding nodes in adjacent layers. G is the intralayer coupling matrix that governs the interaction among nodes within the same layer and $A_{i,j}^{l} = 1$ if i, j are connected by an edge, otherwise zero ($l = 1, 2, 3$). The intralayer connections are considered as global network through the state variable x for each layer, along with relay type coupling across the layers, i.e., $G = \begin{bmatrix} 1 & 0 & 0 \\ 0 & 0 & 0 \\ 0 & 0 & 0 \end{bmatrix}$ and $H = \begin{bmatrix} 1 & 0 & 0 \\ 0 & 0 & 0 \\ 0 & 0 & 0 \end{bmatrix}$. Subsequently, we perform the simulation of system (14) for $N = 100$ oscillators in each layer using the RK-45 method for a specified global coupling strength of $\mu = 0.3$ with all the same initial condition of state variables as Sec. 2.1 We observe same result occurs like Fig. 2 when we add mismatch $\Delta w = 0.1$ and $\Delta w = 0.2$ in the relay layer. Fig. 7 also confirms these statements. In this parameter region, we can see that there is sharp transition from high values of the synchronization error (yellow region) to low synchronization error (blue region). This is a clear signature of anomalous complete synchronization phenomena. Therefore, we conclude that the anomalous synchronization remains unchanged when a global connection is incorporated in each layer.

5.2. Global network of coupled Rössler oscillators with time delay

Now, we extend the results for three coupled time delayed Rössler oscillators in Sec. 3 to the network of oscillators. In this section, we

emphasize the impacts of global networking on Rössler oscillators with a time-delay in the interlayer coupling functions. Mathematical form is similar as Eq. (14) only changes in interlayer relay type coupling, instead of $[\mathbf{X}_{2,i}-\mathbf{X}_{1,i}]$, $[\mathbf{X}_{3,i}+\mathbf{X}_{1,i}-2\mathbf{X}_{2,i}]$ & $[\mathbf{X}_{2,i}-\mathbf{X}_{3,i}]$, the time delayed relay type coupling function will be $[\mathbf{X}_{2,i}(t-\tau)-\mathbf{X}_{1,i}]$, $[\mathbf{X}_{3,i}(t-\tau)+\mathbf{X}_{1,i}(t-\tau)-2\mathbf{X}_{2,i}]$ & $[\mathbf{X}_{2,i}(t-\tau)-\mathbf{X}_{3,i}]$. All other parameters and matrix remain same as mention earlier in Sec. 5.1. Initial condition of the state variables and delay time (τ) are same as mentioned previously in Sec. 3. After careful numerical simulation, we observed similar ACS phenomenon in this case as well as shown in Fig. 5 (Separate figure is not shown to avoid redundancy).

6. Conclusions

We discussed the synchronization between two outer oscillators in a chain of three oscillators when they are coupled via the relay oscillator(s). The conventional route to complete synchronization gets disturbed when there is heterogeneity in terms of parameter mismatch in the relay oscillator and a new route emerges, wherein the synchronization error suddenly drifts before gradually ceasing to zero beyond the threshold coupling strength, and we coined the term "Anomalous Complete Synchronization (ACS)" to describe this phenomenon. In the ACS regime, generalized synchronization develops between the relay oscillator and the outer oscillators. We established the result using Lorenz & Rössler oscillators in their chaotic regimes and Ginzburg–Landau limit cycle oscillator and Rössler oscillator with periodic regime (in Appendix). Finally, we prove that the lag synchronization between the relay oscillator and the outer oscillators is the possible regime for ACS. We have analytically derived the region of ϵ for the emergence of the ACS state. We further extended our study of ACS phenomenon for coupled Rössler system in presence of time delay coupling. Finally, we have explored the ACS phenomenon for network of three layers in the form of multiplex configurations. The results may be extended by considering a different system in the relay oscillator and the possible generalized synchronization relation between the relay and the outer oscillators. The real experimental verification of the ACS state and enhancing synchrony could be another interesting research problem in the near future. One of the possible real-world implications could be the verification of complete synchronization of indirectly connected neurons among different parts of brain.

CRediT authorship contribution statement

Ranjib Banerjee: Formal analysis, Methodology, Visualization, Writing – original draft. **Sayan Acharya:** Conceptualization, Formal analysis, Methodology, Software, Visualization, Writing – original draft. **Matjaž Perc:** Conceptualization, Supervision, Visualization, Writing – review & editing. **Dibakar Ghosh:** Conceptualization, Supervision, Visualization, Writing – review & editing.

Code availability

The codes that have been used to report the findings of this study will be made available on request.

Declaration of competing interest

The authors declare that they have no known competing financial interests or personal relationships that could have appeared to influence the work reported in this paper.

Acknowledgement

M.P. was supported by the Slovenian Research and Innovation Agency (Javna agencija za znanstvenoraziskovalno in inovacijsko dejavnost Republike Slovenije) (Grant Nos. P1-0403 and N1-0232).

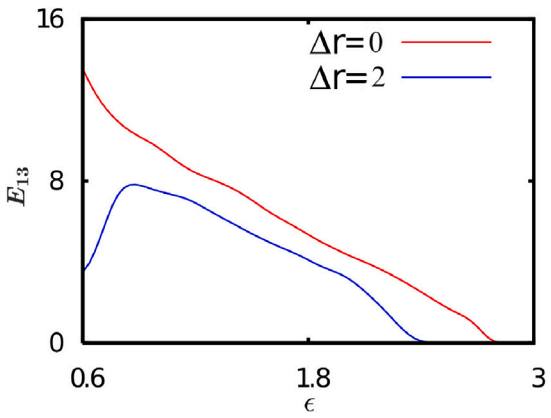

Fig. 8. Anomalous synchronization between the outer oscillators when three Lorenz oscillators are coupled diffusively and the intermediate oscillator has parameter mismatch. $y-axis$ represents for error between outer oscillators and $x-axis$ represents for coupling strength. The red line indicates the synchronization error for parameter mismatch zero ($\Delta r = 0$) and the blue line is used for parameter mismatch equals 2 ($\Delta r = 2$).

Appendix

In this section, we present two examples on chaotic Lorenz systems and periodic Ginzburg–Landau oscillators to verify the ACS states in three coupled oscillators in the open chain (in Fig. 1).

A.1. Chaotic lorenz systems

In this section, we consider the case of three coupled Lorenz oscillators and the coupling configuration remains the same as in Fig. 1 in which the individual dynamics of each of the oscillators is governed by the Lorenz system. The dynamics of the coupled system is given by

Outer oscillators:

$$\begin{aligned}\dot{x}_{1,3} &= \sigma(y_{1,3}-x_{1,3}),\\ \dot{y}_{1,3} &= (\rho-z_{1,3})x_{1,3}-y_{1,3}+\epsilon(y_2-y_{1,3}),\\ \dot{z}_{1,3} &= x_{1,3}y_{1,3}-bz_{1,3},\end{aligned} \tag{15}$$

Relay oscillator:

$$\begin{aligned}\dot{x}_2 &= \sigma(y_2-x_2),\\ \dot{y}_2 &= (\rho+\Delta\rho-z_2)x_2-y_2+\epsilon(y_1+y_3-2y_2),\\ \dot{z}_2 &= x_2y_2-bz_2.\end{aligned} \tag{16}$$

To verify the anomalous behavior in the route to complete synchronization, we introduced mismatch $\Delta\rho$ in ρ in the relay oscillator (Oscillator 2 in Fig. 1). All other parameters are the same for all three oscillators. The choice of parameters ($\sigma = 10, \rho = 28, b = 8/3$) confirms the chaotic dynamics of the uncoupled oscillators. The qualitative behavior of route to the complete synchronization between the outer oscillators in this case is consistent with the behavior found for the case of coupled Rössler oscillators, as discussed previously. The effect of mismatch is graphically summarized in Fig. 8, in which the red color represents the synchronization error for $\Delta\rho = 0$ (when all three oscillators are identical) and the blue line is used to plot the synchronization error for the mismatch case (mismatch is $\Delta\rho = 2$). The ACS effect is clearly evident from the Fig. 8 when there is a mismatch ($\Delta\rho \neq 0$) in the relay oscillator.

A.2. Three linearly coupled limit cycle oscillators

In this section, we consider three linearly coupled Ginzburg–Landau oscillators. Each oscillator can be represented by a system of two

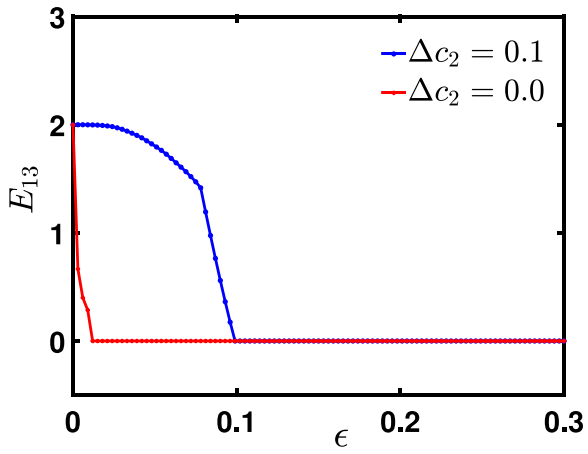

Fig. 9. Anomalous complete synchronization between the outermost oscillators for three coupled Ginzburg–Landau oscillators. Parameter values are $c_1 = 5.5, c_2 = 1.2$. The red line is used for synchronization error E_{13} when $\Delta c_2 = 0$, whereas, the blue line represent synchronization error E_{13} when $\Delta c_2 = 0.1$.

first-order coupled differential equations as defined below.

$$\dot{x} = x - c_1 y - (x - c_2 y)(x^2 + y^2),$$
$$\dot{y} = y + c_1 x - (y + c_2 x)(x^2 + y^2), \tag{17}$$

where c_1, c_2 are the system parameters and x, y are the state variables. Three such oscillators are being mutually coupled using the first state variable (x) and the mismatch has been introduced in the relay oscillator with c_2. Now the dynamics of coupled Ginzburg–Landau oscillators is as follows

Outer oscillators:

$$\begin{aligned}\dot{x}_{1,3} &= x_{1,3} - c_1 y_{1,3} - (x_{1,3} - c_2 y_{1,3})(x_{1,3}^2 + y_{1,3}^2) \\ &\quad + \epsilon(x_2 - x_{1,3}), \\ \dot{y}_{1,3} &= y_{1,3} + c_1 x_{1,3} - (y_{1,3} + c_2 x_{1,3})(x_{1,3}^2 + y_{1,3}^2),\end{aligned}$$

Relay oscillator:

$$\begin{aligned}\dot{x}_2 &= x_2 - c_1 y_2 - (x_2 - (c_2 + \Delta c_2) y_2)(x_2^2 + y_2^2) \\ &\quad + \epsilon(x_1 + x_3 - 2x_2), \\ \dot{y}_2 &= y_2 + c_1 x_2 - (y_2 + (c_2 + \Delta c_2) x_2)(x_2^2 + y_2^2),\end{aligned}$$

where c_1 and c_2 are system parameters, Δc_2 be the amount of mismatch in c_2 and ϵ is the coupling strength. For proper visualization of CS between the outer oscillators, we plot synchronization error E_{13} as a function of coupling strength (ϵ) in Fig. 9. The Fig. 9 shows the anomalous behavior in the route to CS between the oscillators 1&3 due to the presence of parameter mismatch $\Delta c_2 = 0.1$ in the central oscillator, however, in the absence of the mismatch, the outermost oscillators follow the usual path to achieve the stable synchrony. Here time average synchronization error is defined as

$$E_{i,j} = \left\langle \sqrt{(x_i - x_j)^2 + (y_i - y_j)^2} \right\rangle_t, \tag{18}$$

where $\langle \cdots \rangle_t$ denotes the time average. For numerical simulation we use RK-45 method with $t = 10^7$ time iteration and small step size $dt = 0.01$. The time averaged synchronization error E_{13} is calculated using last 20% data and we choose initial condition randomly from $(0, 1)$.

Data availability

Data will be made available on request.

References

[1] Pikovsky A, Rosenblum M, Kurths J. Synchronization: a universal concept in nonlinear science. American Association of Physics Teachers; 2002.
[2] Simeone O, Spagnolini U, Bar-Ness Y, Strogatz SH. IEEE Signal Process Mag 2008;25(5):81–97.
[3] Ji P, Ye J, Mu Y, Lin W, Tian Y, Hens C, et al. Phys Rep 2023;1017:1–96.
[4] Nishikawa T, Motter AE. New J Phys 2015;17(1):015012.
[5] An X-l, Zhang L, Li Y-z, Zhang J-g. Phys A 2014;412:149–56.
[6] Wang Q, Chen G, Perc M. PLoS One 2011;6(1):e15851.
[7] Zhang L, Motter AE, Nishikawa T. Phys Rev Lett 2017;118(17):174102.
[8] Nicosia V, Valencia M, Chavez M, Díaz-Guilera A, Latora V. Phys Rev Lett 2013;110(17):174102.
[9] Bergner A, Frasca M, Sciuto G, Buscarino A, Ngamga EJ, Fortuna L, et al. Phys Rev E 2012;85(2):026208.
[10] Fischer I, Vicente R, Buldú JM, Peil M, Mirasso CR, Torrent M, et al. Phys Rev Lett 2006;97(12):123902.
[11] Gao R, Lu Z, Liu Z. Chaos Solitons Fractals 2024;186:115223.
[12] Vlasov V, Bifone A. Sci Rep 2017;7(1):10403.
[13] Gambuzza LV, Cardillo A, Fiasconaro A, Fortuna L, Gómez-Gardenes J, Frasca M. Chaos: An Interdiscip J Nonlinear Sci 2013;23(4):043103.
[14] Rakshit S, Parastesh F, Chowdhury SN, Jafari S, Kurths J, Ghosh D. Nonlinearity 2021;35(1):681.
[15] Anwar MS, Ghosh D, Frolov N. Mathematics 2021;9(17):2135.
[16] Banerjee R, Ghosh D, Padmanaban E, Ramaswamy R, Pecora L, Dana SK. Phys Rev E 2012;85(2):027201.
[17] Banerjee R, Bera BK, Ghosh D, Dana SK. Eur Phys J Spec Top 2017;226:1893–902.
[18] Blasius B, Montbrió E, Kurths J. Phys Rev E 2003;67(3):035204.
[19] Ataka M, Ohta T. Progr Theoret Phys 2005;113(1):55–62.
[20] Dana SK, Blasius B, Kurths J. AIP conference proceedings, vol. 742, no. 1. American Institute of Physics; 2004, p. 69–74.
[21] Prasad A, Kurths J, Ramaswamy R. Phys Lett A 2008;372(40):6150–4.
[22] Tokuda IT, Dana SK, Kurths J. Chaos: An Interdiscip J Nonlinear Sci 2008;18(2):023134.
[23] Dayani Z, Parastesh F, Nazarimehr F, Rajagopal K, Jafari S, Schöll E, et al. Chaos: An Interdiscip J Nonlinear Sci 2023;33(3):033139.
[24] Boccaletti S, Kurths J, Osipov G, Valladares D, Zhou C. Phys Rep 2002;366(1–2):1–101.
[25] Rakshit S, Ghosh D. Chaos: An Interdiscip J Nonlinear Sci 2020;30(11):111102.
[26] Gutierrez R, Sevilla-Escoboza R, Piedrahita P, Finke C, Feudel U, Buldu JM, et al. Phys Rev E 2013;88(5):052908.
[27] Hale J. Delay Differ Equ Appl 2006;1–28.
[28] Asl FM, Ulsoy AG. J Dyn Syst, Meas Control 2003;125(2):215–23.
[29] Cooke KL. International symposium on nonlinear differential equations and nonlinear mechanics. Elsevier; 1963, p. 155–71.
[30] Gorechi H, Fuksa S, Grabowski P, Korytowski A. Analysis and Synthesis of Time Delay Systems. Elsevier; 1991.
[31] Egorov A. IFAC-PapersOnLine 2019;52(18):85–90.
[32] Yi S, Ulsoy AG, Nelson PW. Proceedings of the 45th IEEE conference on decision and control. IEEE; 2006, p. 2535–40.
[33] Mackey MC, Glass L. Science 1977;197(4300):287–9.
[34] Ghosh D, Grosu I, Dana SK. Chaos: An Interdiscip J Nonlinear Sci 2012;22(3):033111.
[35] Pyragas K. Phys Rev E 1998;58(3):3067.